

Intruder clustering in three-dimensional granular beds

L. T. Lui, Michael R. Swift, R. M. Bowley, and P. J. King

School of Physics and Astronomy, University of Nottingham, Nottingham, NG7 2RD, United Kingdom

(Received 17 November 2006; published 4 May 2007)

We present results of computer simulations for neutrally buoyant intruders in a vertically vibrated three-dimensional granular bed of smaller host particles. Under sinusoidal excitation, pairs of intruders interact over a distance of several intruder diameters; a group of intruders forms a cluster. The strength of the interaction grows as the number of intruders is increased. We show that the tendency to cluster may be manipulated through the use of nonsinusoidal excitation, which allows partial mixing. Finally, we investigate the effects of walls on the clustering of intruders.

DOI: [10.1103/PhysRevE.75.051303](https://doi.org/10.1103/PhysRevE.75.051303)

PACS number(s): 45.70.-n, 45.70.Mg

I. INTRODUCTION

Granular materials are widespread in nature and in commerce, where granular mixtures have myriad uses. The manipulation of granular mixtures through various forms of vibration has many important scientific and technological applications [1,2]. Consequently, there has long been an interest in the behavior of large “intruders” within a granular bed excited by tapping or by periodic vertical vibration [3]. A single intruder may exhibit the Brazil nut effect, moving to the top of the host bed under vibration, or it may exhibit the reverse Brazil nut effect, moving to the bottom of the bed. Which of the two occurs depends upon the size and density of the intruder and host particles [4]. These Brazil nut effects are due to the interaction between the intruder and the host grains during the excitation. The question then arises as to whether there is an interaction between two or more intruders in an excited granular bed [6].

Recently, intruder-intruder interactions have been studied through the use of neutrally buoyant intruders in two-dimensional (2D) granular beds [6,7]. The density of the intruders may be adjusted so that, over a wide range of vibratory conditions, they remain on average at mid-bed height [5]. In 2D it has been shown in both simulation and experiment that, under sinusoidal excitation, neutrally buoyant intruders display an attractive interaction which has a range of about five intruder diameters [6,7]. An explanation has been given based on the relative sizes of the intruder attraction and repulsion found over various phases of the vibration cycle [6]. For sinusoidal excitation there is a net attraction. However, the relative sizes of the attraction and repulsion can be controlled by the use of a nonsinusoidal wave form [8]. Suitable wave forms may be used to reduce the net attraction sufficiently so that it is close to zero.

Here we describe the interaction of neutrally buoyant intruders in a vertically vibrated 3D granular bed. We show, through the use of molecular dynamics simulations, that intruders are attracted to each other when the bed is shaken sinusoidally. The strength and range of the attraction vary with the number of intruders, the interaction becoming stronger for larger intruder numbers. We demonstrate that the strength of the intruder-intruder interaction may be controlled through manipulation of the vibratory wave form. Finally, we consider the influence of walls on the intruder be-

havior. We show that the intruders are attracted to the walls and corners of the container in which they are vibrated. Our findings may have significant implications concerning the separation or mixing of granular materials.

II. SIMULATION DETAILS

Our simulations use soft-sphere molecular dynamics to describe a vibrated granular bed [9]. Initially we consider sinusoidal vertical excitation of the container, $z_c = A \sin(\omega t)$, which has a maximum acceleration with respect to gravity $\Gamma = A\omega^2/g$. We simulate a system of 16 000 spherical host particles of mass 4.2×10^{-6} kg and diameter 2 mm, which are contained within a rectangular cell with horizontal dimensions 80×80 mm². The granular bed is therefore approximately 10 host particle diameters deep at rest and 12–14 diameters deep when shaken in the manner which we shall describe. The bed also contains a small number of spherical intruder particles which have a diameter of 6 mm and a mass of 8.5×10^{-5} kg.

The particles interact through a linear spring-dashpot force [10]. The spring constant was chosen to be 1000 N m⁻¹ while the damping was adjusted to correspond to a coefficient of normal restitution of 0.9, for host-host, intruder-intruder, and host-intruder collisions. Tangential friction and particle rotation have both been ignored, a simplification which is not expected to change the behavior of the system significantly [11]. Although we have chosen to simulate a system with a particular form of interaction and a particular set of parameters, we believe that the key effects that we have observed are relatively insensitive to small changes in these details.

Initially we describe results from a system with periodic boundary conditions in the horizontal directions: whenever a particle crosses a boundary its position is adjusted to that of the equivalent position on the far side of the cell.

III. BEHAVIOR UNDER SINUSOIDAL VIBRATION

We first consider the behavior of a single intruder in a bed vibrated at 30 Hz and with Γ in the range 4–6.5. The intruder is neutrally buoyant (the mean height is equal to about half the bed depth) for the densities chosen above and for this range of Γ . The standard deviation of the height fluctua-

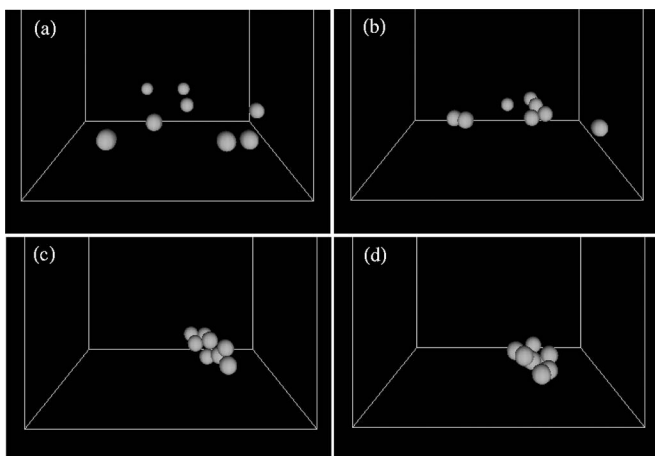


FIG. 1. Series of snapshots showing the time evolution of eight intruders vibrated at 30 Hz and with $\Gamma=4$. For clarity, the host particles are not shown. From top left to bottom right, the images show the configuration after times (a) 0, (b) 240, (c) 360, and (d) 520 s.

tions is about 0.26 intruder diameters. This is appreciably smaller than the height deviation in an equivalent 2D system [6,7]. In our 3D system neither the mean height nor the standard deviation in height varies strongly with Γ , within the range of Γ values used. The resulting motion of the intruder is predominantly two dimensional, the intruder moving randomly in the horizontal plane. As Γ is reduced below 4, the time scale for intruder movement becomes increasingly long and the simulations become more difficult. It should be noted that, in our system, neutral buoyancy occurs when the intruder density is about 3/4 of the material density of the host particles. For vertically vibrated beds, this ratio does not correspond exactly to that predicted purely from Archimedeian buoyancy since temporal and spatial fluctuations in the bed are important [3–6].

We next consider the behavior of N such intruders in the bed that is vibrated at 30 Hz and with $\Gamma=4$. We find that for these conditions multiple intruders exhibit clustering behavior. Figure 1 shows snapshots of eight intruders: initially, the intruders were positioned randomly within the bed; after a short time the intruders can be seen to form small groups; later, these groups come together until all eight intruders form a tightly bound cluster which remains stable for all subsequent times, moving like a swarm of angry bees meandering about the cell. The cluster is, on the average, slightly more extended in the horizontal x - y plane than in the vertical z direction.

In order to study the clustering behavior in more detail, simulations were run for an extended period of time, and the positions of the intruders were noted once per cycle, when the base is at its lowest point. Our simulations show that the intruders move very little during each cycle, so that the choice of when in the cycle the positions are measured is unimportant.

First, we calculate the probability distribution $p_N(r)dr$ of finding any two intruders separated by a distance between r and $r+dr$. We have used r rather than the separation in the x - y plane since the intruder cluster has an extension in the z

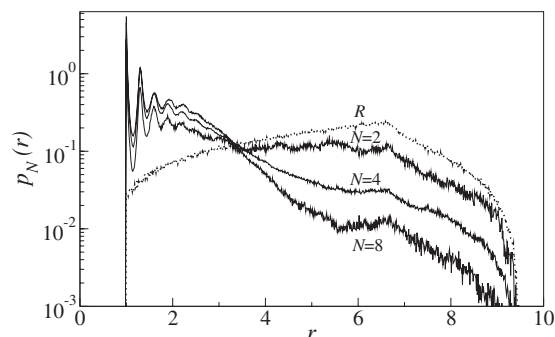


FIG. 2. Pair probability function $p_N(r)$ as a function of r for $N=2, 4$, and 8 intruders, for a bed vibrated at 30 Hz with $\Gamma=4$. The line labeled R corresponds to the pair probability function for two noninteracting intruders and is further described in the text.

direction. Figure 2 shows the resulting data for $N=2, 4$, and 8 intruders. In this, and all similar figures, the distance r is presented in units of intruder diameters. At small distances, each curve displays oscillatory structure resulting from depletion effects, the spacing between peaks corresponding to the diameter of the host particles [6,12]. As the number of intruders increases, the weight of the distribution shifts to shorter distances. This implies an increased attractive interaction between intruders as the number of intruders increases.

These distributions may be compared with the form of $p_N(r)$ expected for two noninteracting intruder particles, shown in Fig. 2 as the line labeled R . This distribution is readily obtainable in simulation by placing two intruders at random in the bed, subject to the constraint that they do not overlap; this process is repeated very many times until an accurate distribution is obtained. It is noteworthy that, at low r , this distribution rises with r ; the pronounced kink at $r \approx 6.7$ and the subsequent reduction of $p_N(r)$ to zero at $r \approx 9.5$ are a consequence of the system size we have used and the imposition of periodic boundary conditions. The kink at $r \approx 6.7$ is weakly reflected in each of the data curves which we have shown. The difference between the overall forms of the random distribution R and the pair probability distribution function for $N=2$ clearly shows that even two intruders are attracted to each other.

The quantity $p_N(r)$ represents one measure of clustering. We may also define a measure of clustering by the mean intruder separation,

$$\bar{r} = \frac{2}{N(N-1)} \sum_{i=1}^N \sum_{j>i}^N |\mathbf{r}_i - \mathbf{r}_j|, \quad (1)$$

where \mathbf{r}_i is the position of intruder i . For a given number of intruders, N , we calculate \bar{r} each time the base of the cell is at the lowest point. Figure 3 shows the mean separation between eight intruders as a function of time. Initially the intruders were randomly placed in the system; the value of the mean intruder separation \bar{r} is then around 5.5. After about 170 s the value of \bar{r} dropped to around 2, indicating that the intruders are closely packed together and a cluster has

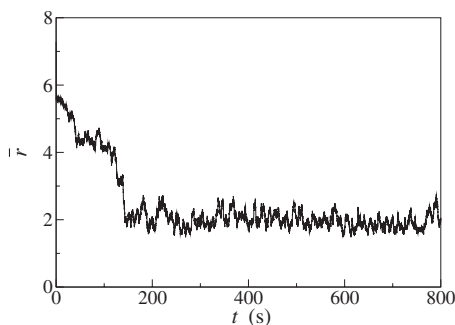


FIG. 3. Time evolution of \bar{r} for eight intruders vibrated at 30 Hz with $\Gamma=4$. After a time of about 170 s, a cluster is formed which remains stable.

formed. Once the intruders formed a cluster they remain clustered for the rest of the simulation.

Several simulations were run. The initial transients, the first 200 s, were ignored, and then both a time average and an ensemble average over different runs were carried out. From the \bar{r} values sampled we generated a probability distribution $q_N(\bar{r})d\bar{r}$ of finding an average spacing in the range \bar{r} to $\bar{r}+d\bar{r}$ with $d\bar{r}=0.05$ intruder diameters. These distributions for four, eight, and 16 intruders are plotted in Fig. 4. Each curve shows the existence of clustering. The probability distribution $q_N(\bar{r})$ becomes more peaked as the number of intruders increases, indicating that the more particles which are present, the stronger the clustering. There is a shift of the peak toward higher values of \bar{r} as N increases: once a tightly formed cluster has formed, extra particles can attach themselves only on the outer surface of the cluster, which makes the cluster size increase.

Figure 5 shows $q_N(\bar{r})$ for eight intruders vibrated at 30 Hz for different values of Γ . As Γ increases, the distribution broadens and shifts to larger values of \bar{r} . For comparison we show the equivalent distribution for the random placement of eight intruders, with no two intruders overlapping. From the form of these curves it can be seen that, as Γ increases, the tendency to cluster weakens.

All our measures confirm that there is an attractive interaction between intruders for sinusoidal vibration of the system, with Γ in the range 4–6. Intruder-intruder interactions

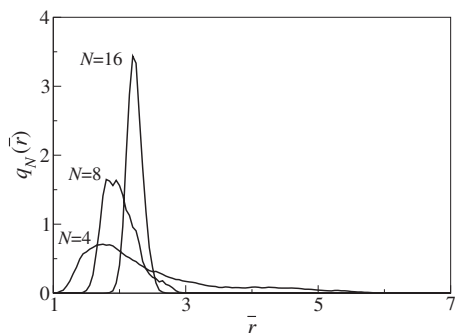


FIG. 4. Cluster size probability function $q_N(\bar{r})$ as a function of \bar{r} for $N=4, 8$, and 16 intruders, for a bed vibrated at 30 Hz with $\Gamma=4$. The narrowing of the probability distribution as the number of intruders increases implies that the cluster is more tightly bound.

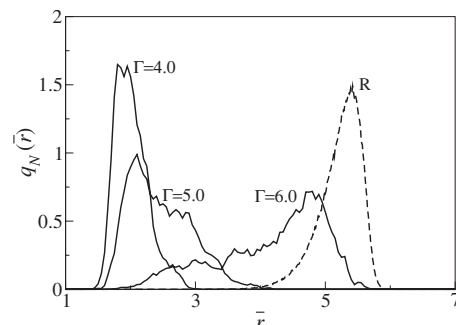


FIG. 5. Cluster size probability function $q_N(\bar{r})$ for different values of Γ with eight intruders vibrated at 30 Hz. The dashed curve labeled R corresponds to the random placement of eight intruders in the bed. As Γ is increased, the tendency to cluster diminishes.

mediated by host particles have been observed in a number of systems [6,12–16]. In each case, the interactions arise through the modification of the host-particle behavior by the presence of the intruders. In the situation studied by Duran *et al.* [13], the interaction force is provided by dislocations in a crystallised host bed. This mechanism is applicable only at very low values of Γ . A very short-range attraction also occurs when two intruders are sufficiently close to each other that host particles are excluded from the volume between them [12]. Longer-range forces may occur in the more general situation where the presence of the intruders causes the density and/or granular temperature between them to be different from that in the bulk of the bed [6,14–16]. The resulting differential pressure of the host particles on the intruders provides the interaction.

In the case of a vertically vibrated bed, Sanders *et al.* [6] have found that this longer-range force may be attractive and repulsive at different phases of the cycle. As the bed is thrown, host particles are forced between the intruders, leading to a repulsion. However, as the bed is landing, the reduced host particle density between intruders leads to an effective attraction. For sinusoidal vibration, there is a net attractive interaction. Sanders *et al.* have shown that in 2D modification of the wave form can then be used to control the balance between the attractive and repulsive components of the interaction [8]. Here we investigate a similar behavior in 3D vertically vibrated beds.

IV. THE INFLUENCE OF NONSINUSOIDAL EXCITATION

One of the effects found in two-dimensional systems is that clusters can be broken up by using a modified wave form [8]. To find out if this happens in a three-dimensional system, we oscillated the base of the cell as

$$z_c(t) = A_1 \sin(\omega t) + A_2 \sin(2\omega t + \phi), \quad (2)$$

with $\omega/2\pi=30$ Hz and $A_2=0.5A_1$. For a range of values of A_1 , it was observed that the bed became markedly less fluidized for ϕ in the range 80° – 180° . To compensate for this variation, for each ϕ we scaled A_1 and A_2 by a numerical factor in such a way that the bed appeared to have roughly the same degree of fluidity as for a sinusoidally vibrated bed

TABLE I. The values of amplitude A_1 and the corresponding value of T_g for different values of ϕ . We adjusted the values of A_1 , keeping $A_2=0.5A_1$, in order to fix T_g at approximately $0.0342 \text{ m}^2 \text{ s}^{-2}$.

ϕ (deg)	A_1 (mm)	T_g ($\text{m}^2 \text{ s}^{-2}$)
0	0.680	0.0342
30	0.691	0.0342
60	0.724	0.0336
90	0.884	0.0346
120	1.176	0.0334
150	1.347	0.0334
180	1.191	0.0338
210	1.036	0.0334
240	0.905	0.0346
270	0.785	0.0340
300	0.723	0.0342
330	0.691	0.0342

at 30 Hz with $\Gamma=4.5$. To make this more precise we calculated the variance of the velocity fluctuations of the host particles relative to the bed's center of mass, which is given by

$$T_g = \frac{1}{N_h} \sum_{i=1}^{N_h} \overline{[\mathbf{u}_i(t) - \mathbf{v}(t)]^2}. \quad (3)$$

Here N_h is the number of host particles, $\mathbf{u}_i(t)$ is the velocity of host particle i at time t , $\mathbf{v}(t)$ is the average velocity of the bed, and the overbar indicates a time average over many cycles, taking samples 20 times per cycle. By adjusting A_1 , keeping $A_2=0.5A_1$, we were able to keep T_g within about $\pm 1\%$ of $0.0342 \text{ m}^2 \text{ s}^{-2}$. The values chosen are given in Table I. For all these values, the intruders remain neutrally buoyant and mobile in the bed.

The simulation was run for eight intruders and the phase ϕ varied. In Fig. 6 we show the variation of the average

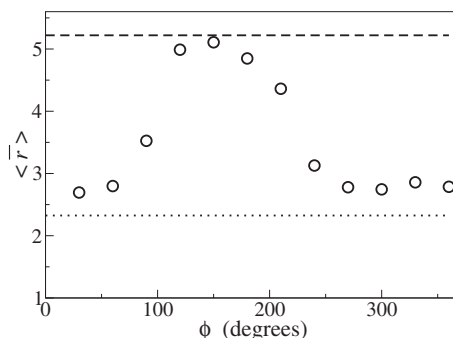


FIG. 6. Mean separation $\langle \bar{r} \rangle$ as a function of ϕ for eight intruders. For ϕ in the range 120° – 150° , $\langle \bar{r} \rangle$ is close to the value obtained for random placements of intruders, shown by the dashed line. The lower, dotted line corresponds to $\langle \bar{r} \rangle$ for sinusoidal oscillation at 30 Hz with the same T_g as used for nonsinusoidal vibration, conditions for which clustering is observed.

value of \bar{r} as a function of ϕ . The value of \bar{r} over the range $\phi=120^\circ$ – 150° is a maximum. For these angles it is tempting to believe that the cluster is completely broken apart. To test this idea, we calculated the average value of \bar{r} for eight intruders if they are placed at random in the cell, subject to the constraint that no two intruders overlap. It is easy to determine \bar{r} by means of a computer simulation: each intruder was placed roughly halfway up the bed, but with random x and y coordinates; if none of the intruders overlap, the set of coordinates x_i , y_i , and z_i for the eight intruders is retained; if not the process is repeated, until an ensemble of $M=10^4$ such sets of coordinates have been generated. From each of the M sets we can generate \bar{r} ; from the M values of \bar{r} we can calculate the average $\langle \bar{r} \rangle$, which turns out to be approximately 5.2. This is shown as the upper dashed line in Fig. 6. For ϕ in the range $\phi=120^\circ$ – 150° , the measured $\langle \bar{r} \rangle$ is indeed very close to that obtained for randomly placed intruders. For comparison, the value of $\langle \bar{r} \rangle$ for a sinusoidally oscillated system with the same T_g as in the nonsinusoidal case is shown as the lower dotted line.

A more sensitive test for the absence of clustering, based on the use of two-dimensional Fourier transforms, is described in the Appendix. The advantage of this measure is that it allows a sensitive comparison between a weakly clustered system and a random placement of nonoverlapping intruders. As a result we are confident that for ϕ in the range 120° – 150° , the intruders behave as if they were randomly placed in the bed, subject to the constraint that no two intruders overlap.

It is interesting to examine the wave form for values of ϕ for which clustering and non-clustering is observed. In Fig. 7(a) we show as a dashed line the position of the base of the cell and as a solid line the position of the bottom of the bed, through a complete cycle of vibration. The height of the bottom of the bed was determined by averaging the height of the lowest 400 host particles (approximately one layer), less the radius of a host particle. The simulation is for $\phi=300^\circ$, a phase angle for which clustering is observed. During each cycle the bed is thrown from the base of the cell and subsequently experiences a “soft landing” in which the base of the cell moves downward while in contact with the bottom of the bed. This process lasts over an extended period of a cycle. In Fig. 7(a) it occurs from about 40° to 150° . The bed is then at rest on the platform and is thrown again later in the cycle. The overall trajectory of the bed is similar to the one observed in the case of pure sinusoidal oscillation. In contrast, in Fig. 7(b), which is for $\phi=150^\circ$, where clustering is absent, the bed is thrown twice in rapid succession. Subsequently it experiences a “hard landing” with the upward moving platform before being thrown again. Note that the amplitude of oscillation of the base of the cell is quite different in the two cases; however, the resulting amplitude of motion of the base of the bed is roughly the same. The intruder behavior is completely different in the two cases despite the bed amplitude of motion and T_g being the same.

From a detailed investigation of similar figures for other values of ϕ , it seems that nonclustering occurs over the narrow range of angles where the bed is thrown twice per cycle and experiences a hard landing. A similar dependence of

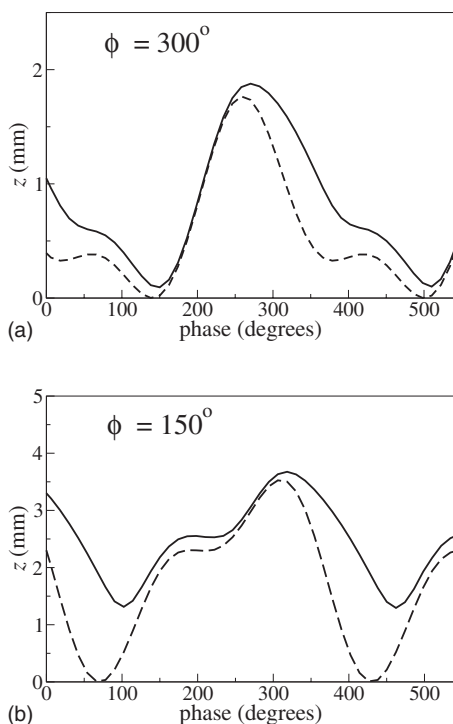


FIG. 7. Variation of the height of the bottom of the bed (solid line) and the base of the cell (dashed line) through a cycle of oscillation. (a) shows the behavior for $\phi=300^\circ$, a phase angle for which the intruders cluster. (b) is for $\phi=150^\circ$, a phase angle for which clustering is absent. The heights shown are measured from the lowest position of the base of the cell.

clustering on the vibratory wave form has been observed experimentally in 2D shaken beds [8]. This suggests that the mechanism for the interaction in 3D is similar in nature to that in 2D [6,8], and that changing the wave form alters the balance between the attractive and repulsive components of the force provided by the host particles at different times during the vibratory cycle.

It is possible to switch directly between sinusoidal and nonsinusoidal wave forms, both of which correspond to the same T_g , to see whether a cluster can be broken up. Here we consider a value of T_g that corresponds to sinusoidal vibration at 30 Hz with $\Gamma=4.3$. We ran the simulation for $\phi=150^\circ$ and measured \bar{r} as a function of time. Initially the intruders were placed at random and subjected to the nonsinusoidal wave form; at 500 s the wave form was altered to the sinusoidal form with the same T_g . The value of \bar{r} decreases as shown in Fig. 8; at 1000 s the wave form was changed back to the original nonsinusoidal wave form, whereupon the value of \bar{r} increased back to the previous value corresponding to nonclustered particles. The lower line in Fig. 8 shows how T_g varies with time; it is constant except at the points where the wave form changes. The transition is repeatable with no sign of hysteresis: the system can be changed from a strongly clustered state to a less clustered state simply by switching the wave form.

V. REFLECTIVE WALLS

So far we have considered a system with periodic boundary conditions in the x and y directions. Now we turn to the

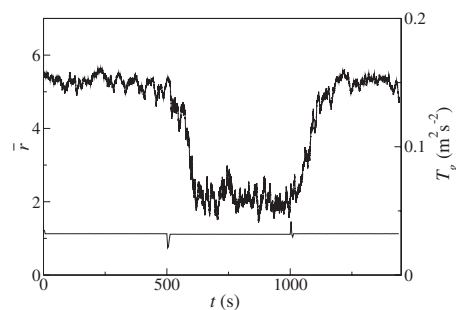


FIG. 8. \bar{r} versus time for a system that switches from nonsinusoidal to sinusoidal wave forms and back again. The lower line shows T_g , which is the same for the two wave forms.

case where the walls of the system specularly reflect the particles. It is straightforward to repeat the computer simulations with boundary conditions that correspond to specularly reflective walls: the angle of incidence is equal to the angle of reflection from the wall and the process is elastic. Such boundary conditions avoid complexities associated with granular convection.

When the system is shaken sinusoidally the intruders eventually form a cluster, as suggested in the earlier sections. However, when the intruders approach a wall they move toward it, which indicates that there is an attraction between the walls and the intruders. When the intruders are near a corner they experience an attraction from two directions (two walls) which keep them near the corner. Eventually a cluster forms in the corner.

When the system is shaken nonsinusoidally, the intruders spread out in the system and do not form a cluster. When they arrive at a wall they stay there and move along the walls. There is little tendency to form a cluster in a corner. These simulation results suggest that, when the system is shaken sinusoidally, the intruders will gather at the corners of the cell; and when shaken nonsinusoidally for particular values of ϕ , they will spread out along the walls of the cell.

To illustrate this type of behavior, Fig. 9 presents a succession of snapshots of the system with 64 intruders. The system was first shaken sinusoidally for 500 s at $\Gamma=4.3$. The wave form was then changed to nonsinusoidal, as described by Eq. (2) with $\phi=150^\circ$, and with the same T_g as in this sinusoidal case. This wave form was then applied for another 500 s. With this nonsinusoidal wave form, no cluster should form in the bulk. In the first 500 s when the sinusoidal wave form is applied, the intruders form a cluster, then gather at the walls, and finally congregate near the corners. This is shown in the first three panels of Fig. 9. During the next 500 s, when the nonsinusoidal wave form is applied, the cluster breaks up and the intruders spread out along the walls, as shown in the lower three panels of Fig. 9. This shows that the attraction with the walls is always present, even for a wave form where no cluster forms in the bulk. If the system is shaken sinusoidally again, the intruders will reform clusters at a nearby corner.

VI. CONCLUSIONS

We have studied the behavior of neutrally buoyant intruders in three-dimensional granular systems using molecular

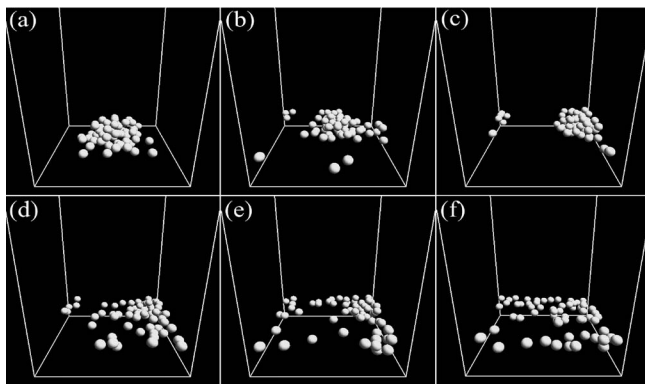


FIG. 9. Snapshots of intruder behavior in a box with reflective boundaries. The top three pictures are for intruders shaken by sinusoidal vibration at 30 Hz and for $\Gamma=4.3$. They correspond to times of (a) 0, (b) 260, and (c) 380 s. The images show that when the intruders are subjected to sinusoidal vibration they remain clustered, and gradually move to one of the corners. The bottom three pictures are taken at times of (d) 650, (e) 760, and (f) 940 s, where the system is vibrated nonsinusoidally with the same T_g . Under these conditions the intruders move away from each other. However, they are still slightly attracted to the walls and spread out along them.

dynamics simulations. Under sinusoidal vibration, for a range of values of Γ , the intruders cluster together; the strength of the interaction grows as the number of intruders increases. If a second harmonic with arbitrary phase is added to the wave form, the clustering of the intruders can be reduced for a suitable choice of amplitude and phase. Indeed, for a particular range of phase angles, the intruders behave as though they are noninteracting. In the final section reflective walls were applied to the system; the intruders are then attracted to the walls. This attraction is present for both sinusoidal and nonsinusoidal excitation.

Our findings have implications for the manipulation of granular mixtures. We have shown that in general there is a natural tendency for neutrally buoyant intruders to cluster. Using a suitably chosen wave form, the intruders can be made to spread out within the bed, a first step toward creating a perfect granular mixture. However, our simulations also indicate that the intruder motion is confined within a range of heights in the bed, limiting the degree of mixing that can be achieved. We have also show that when walls are present, there is a strong tendency to cluster at the walls, again limiting the degree of mixing in practical situations. It would be interesting to test these predictions experimentally and to explore the influence of other wave forms on intruder behavior. However, it is important to note that the effects which we have studied may be in competition with granular convection, and would only be influential if the latter effect was weak.

APPENDIX

As a measure of clustering, the mean spacing of intruders \bar{r} loses its precision if the clustering is weak. In an infinite system, a collection of intruders that interact weakly could

have a value of \bar{r} that is quite large. In a simulation in which the size of the cell is smaller than this value of \bar{r} , the intruders will appear to be randomly placed and therefore not clustered. What we need is a measure that can give an indication of whether weak clustering is present in a system with periodic boundary conditions. We can create such a measure by using a discrete Fourier transform. The advantage of this technique is that the resulting *distribution* can be compared to that obtained by random positioning of the nonoverlapping intruders. If the distributions are the same, this is stronger evidence for the absence of clustering than simply comparing the values of \bar{r} .

From the set of positions x_i, y_i of particles at a given time in the cycle, we can create a two-dimensional Fourier transform with wave vectors $k_x=2\pi n_x/L$ and $k_y=2\pi n_y/L$, with L the length of a side of the box and n_x and n_y integers. (It is not worth including the z variation in the Fourier transform as the intruders remain at roughly the same level.) Then, by time averaging after the initial transients have died away, we can construct

$$S(n_x, n_y) = \left\langle \frac{1}{N} \sum_{i=1}^N \sum_{j=1}^N \exp(i\alpha) \right\rangle, \quad (\text{A1})$$

where

$$\alpha = \frac{2\pi}{L} [n_x(x_i - x_j) + n_y(y_i - y_j)]. \quad (\text{A2})$$

Here the angular brackets $\langle \dots \rangle$ denote both a time average and an average over several different runs.

If the intruders are clustered together $S(n_x, n_y)$ should have a finite value for small values of n_x and n_y , such as $S(1, 0)$, $S(0, 1)$, and $S(1, 1)$. As L tends to infinity the quantity $S(n_x, n_y)$ decreases smoothly from its maximum value $S(0, 0)$ as n_x or n_y increases. The full width at half height of $S(n_x, 0)$ defines a width Δk_x ; the reciprocal of this width is proportional to the radius of the cluster. For finite L we can make a crude estimate of Δk_x providing the radius of the cluster is smaller than L .

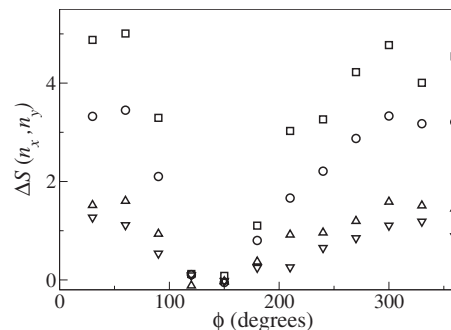


FIG. 10. Difference between S and S_{rand} as a function of ϕ . The squares are for $n_x^2+n_y^2=1$, the circles for $n_x^2+n_y^2=2$, the upward-pointing triangles for $n_x^2+n_y^2=4$, and the downward-pointing triangles for $n_x^2+n_y^2=5$. It can be seen that for ϕ in the range 120° – 150° the difference is effectively zero, indicating the absence of clustering.

When the clustering becomes weaker, the cluster size grows and becomes larger than L . In the extreme limit there is no clustering, and the intruders appear to behave as if they were placed randomly in the cell subject to the constraint that no two intruders overlaps. It is fairly easy to estimate $S(n_x, n_y)$ for this state by means of a computer simulation. Each intruder is placed roughly halfway up the bed, but with random x and y coordinates. If none of the intruders overlap, the set of coordinates X_i , Y_i , and Z_i for the N intruders is retained; if not the process is repeated, until an ensemble of $M=10^4$ such sets of coordinates have been generated. From this procedure we determine $S_{\text{rand}}(n_x, n_y)$ using Eqs. (A1) and (A2) with x_i replaced by X_i and y_i replaced by Y_i . The calculation ignores complexities concerning the configurations

of host particles around intruders, particularly those configurations where two intruders are very close together, say of order a host-particle diameter. Therefore we expect our computer simulation to contain a small error in our estimate of $S_{\text{rand}}(n_x, n_y)$ for large $n_x^2 + n_y^2$.

If, for all n_x, n_y , the difference $\Delta S(n_x, n_y) = S(n_x, n_y) - S_{\text{rand}}(n_x, n_y)$ is zero within the statistical error of our computer simulation [and the systematic error in our estimate of $S_{\text{rand}}(n_x, n_y)$], then the intruders can be said to be randomly placed. In Fig. 10 we show the variation of $\Delta S(n_x, n_y)$ with ϕ for $N=8$ intruders, vibrated with the wave form given by Eq. (2) and the parameters in Table I. It can be seen that for $\phi = 120^\circ$ and 150° all the values of $\Delta S(n_x, n_y)$ are close to zero, indicating that the clustering, if present, is extremely weak.

-
- [1] B. A. Wills, *Mineral Process Technology* (Butterworth and Heinmann, London, 1997).
- [2] For a review, see A. Kudrolli, Rep. Prog. Phys. **67**, 209 (2004), and references therein.
- [3] For a review, see A. D. Rosato *et al.*, Chem. Eng. Sci. **57**, 265 (2002), and references therein.
- [4] D. C. Hong, P. V. Quinn, and S. Luding, Phys. Rev. Lett. **86**, 3423 (2001); N. Shishodia and C. R. Wassgren, *ibid.* **87**, 084302 (2001); A. P. J. Breu, H. M. Ensner, C. A. Kruelle, and I. Rehberg, *ibid.* **90**, 014302 (2003).
- [5] D. A. Huerta and J. C. Ruiz-Suárez, Phys. Rev. Lett. **92**, 114301 (2004).
- [6] D. A. Sanders, M. R. Swift, R. M. Bowley, and P. J. King, Phys. Rev. Lett. **93**, 208002 (2004).
- [7] D. A. Sanders, M. R. Swift, R. M. Bowley, and P. J. King, Europhys. Lett. **73**, 349 (2006).
- [8] D. A. Sanders, M. R. Swift, R. M. Bowley, and P. J. King, Appl. Phys. Lett. **88**, 264106 (2006).
- [9] For a review, see H. J. Herrmann and S. Luding, Continuum Mech. Thermodyn. **10**, 189 (1998).
- [10] S. Yuu, T. Saitoh, and T. Umekage, Adv. Powder Technol. **6**, 259 (1995).
- [11] S. McNamara and S. Luding, Phys. Rev. E **58**, 2247 (1998).
- [12] P. Melby, A. Prevost, D. A. Egolf, and J. S. Urbach, e-print arXiv:cond-mat/0507623.
- [13] J. Duran, J. Rajchenbach, and E. Clément, Phys. Rev. Lett. **70**, 2431 (1993).
- [14] I. Zurriguel, J. F. Boudet, Y. Amarouchene, and H. Kellay, Phys. Rev. Lett. **95**, 258002 (2005).
- [15] M. Pica Ciamarra, A. Coniglio, and M. Nicodemi, Phys. Rev. Lett. **97**, 038001 (2006).
- [16] C. Cattuto, R. Brito, U. M. B. Marconi, F. Nori, and R. Soto, Phys. Rev. Lett. **96**, 178001 (2006).